Heliyon 9 (2023) e21995

Contents lists available at ScienceDirect

Heliyon

journal homepage: www.cell.com/heliyon

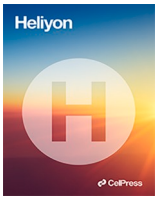

Optimal pretreatment of plantain peel waste valorization for biogas production: Insights into neural network modeling and kinetic analysis

Chinenyenwa Nkeiruka Nweke [a], Chijioke Elijah Onu [a,**], Joseph Tagbo Nwabanne [a], Paschal Enyinnaya Ohale [a,*], Emeka Michael Madiebo [a], Monday Morgan Chukwu [b,***]

[a] Department of Chemical Engineering, Nnamdi Azikiwe University, P.M.B. 5025, Awka, Anambra State, Nigeria
[b] Department of Chemical Engineering, University of Agriculture, Umuagwo, Imo state, Nigeria

ARTICLE INFO

Keywords:
Plantain peels
Anaerobic digestion
Biogas production
Kinetics
Modeling
Optimization

ABSTRACT

This work proposed a model for the substrate treatment stage of biogas production process in an anaerobic digestion system. Adaptive neuro-fuzzy inference system (ANFIS), response surface method (RSM), and artificial neural network (ANN) were comparatively used in the simulation and modeling of the treatment process for improved biogas yield. Waste plantain peels were pretreated and used as substrate. FTIR and SEM results revealed that the pretreatment improved the substrate's desirable qualities. The amount of biogas yield was controlled by time, NaOH concentration, and temperature of the substrate pretreatment. Optimum pretreatment conditions obtained were a temperature of 102.7 °C, time of 31.7 min and NaOH concentration of 0.125 N. RSM, ANN, and ANFIS modeling techniques were proficient in simulating the biogas production, as evidenced by high R^2values of 0.9281, 0.9850, and 0.9852, respectively. Furthermore, the values of the calculated error terms such as RMSE (RSM = 0.04799, ANN = 0.00969, and ANFIS = 0.00587) and HYBRID (RSM = 18.556, ANN = 0.803, and ANFIS = 0.0447) were low, indicating a satisfactory correlation between experimental and predicted values. Scrubbing of the biogas with caustic soda and activated charcoal increased the methane content to 94 %. The kinetics of the cumulative biogas yield were best fit with the Logistics and Modified Logistics models. The low C/N ratio in addition to the presence of potassium, nitrogen, and phosphorus suggested that the spent plantain peel slurry can be utilized as an agricultural fertilizer in crop production. The observations of this study therefore recommends the pre-treatment of biodigestion substrates as a key means to enhance beneficiation of methane production.

* Corresponding author.
** Corresponding author.
*** Corresponding author.
E-mail addresses: cn.nweke@unizik.edu.ng (C.N. Nweke), ce.onu@unizik.edu.ng (C.E. Onu), pe.ohale@unizik.edu.ng (P.E. Ohale), chukwu.monday@uaes.edu.ng (M.M. Chukwu).

https://doi.org/10.1016/j.heliyon.2023.e21995
Received 31 March 2023; Received in revised form 26 October 2023; Accepted 1 November 2023
Available online 3 November 2023
2405-8440/© 2023 The Authors. Published by Elsevier Ltd. This is an open access article under the CC BY-NC-ND license (http://creativecommons.org/licenses/by-nc-nd/4.0/).

Abbreviations/Nomenclature

ANFIS	Adaptive neural fuzzy inference system
RSM	Response surface method
ANN	Artificial neural network
AOAC	Association of Analytical Chemistry
FTIR	Fourier transform infrared
SEM	Scanning electron microscopy
CCD	Central composite design
ANOVA	Analysis of variance
BP	Back-propagation
RMSE	Root mean square error
R^2	Correlation coefficient
ARE	Average relative error
DOE	Design of experiment
PRESS	Predicted sum of squares
CV	Coefficient of variance
APR	Adequate precision ratio
MSE	Mean square error
MLP	multi-layer perceptron
Gaussmf	Gaussian membership function
MF	Membership function
FIS	Fuzzy inference system

1. Introduction

Inadequate waste handling and management are one of the challenges encountered by developing countries [1]. Due to her strides in Agriculture, Nigeria generates huge amount of waste products which are either burnt openly or dumped in drainages, roadsides and other available spaces demystifying and polluting the environment with great damage to the ecosystem [2,3]. The processing and conversion of waste materials into useful products serve a dual purpose in all cases: the elimination/reduction of waste and the synthesis of useful products.

Nigeria is facing environmental challenge due to large solid waste generation. Recently, about 42 million tonnes of wastes were generated in total, according to estimates, with little or no conversion of such waste into useful products and only about 50% of the generated waste being disposed into approved waste bins [2]. This causes environmental pollution and social issues. Most of these wastes are solid wastes. The implementation of waste-to-energy technologies will lead to improvement in solid waste management in developing countries like Nigeria. This includes the production of biogas energy from biomass waste [1].

Bio-degradable biomasses with high organic contents are potential precursors for production of a large volume of biogas via anaerobic digestion process [4,5]. Biomass is a good potential energy source [6]. Examples of biomass which are potential energy sources are solid wastes from agricultural processes, wood, sawdust, straw, seedwaste, manure, paper waste, household wastes, etc. One of such agricultural waste is plantain peel of which Nigeria is one of the world's largest producers [7].

Anaerobic digestion technology can be used to generate biogas from such wastes thereby serving as an alternate energy source while also resolving the environmental pollution challenge [8]. It entails the microbial breakdown of organic materials that will metabolize into biogas or methane in the absence of oxygen [9–11]. The four stages involved in anaerobic digestion are hydrolysis, acidogenesis, acetogenesis, and methanogenesis [12]. The major strength of this anaerobic digestion method is that it transforms agricultural waste materials into energy sources without interfering with the food value chain [13]. Furthermore, the solid organic wastes produced from the anaerobic digestion process can be used as fertilizer and soil amendments [14].

To the increase the amount of biogas production from the process of digestion in the absence of oxygen, the substrate needs to be pretreated. The aim of pre-treating the waste before anaerobic digestion is to make the organic matter in the waste more available to the microorganisms for digestion which will increase the microbial cells and the desirable biogas content [15]. Different pretreatment methods are categorized into physical, chemical, biological, thermal, or a combination of these (physical-chemical and thermo-chemical pretreatment processes), which have proved to yield positive results [15]. Thermo-chemical pretreatment process is a combination of thermal and chemical pretreatment methods [16]. Temperature, concentration of the acid/alkali and time are the factors that influence thermo-chemical pretreatment method. These process factors can be optimized to yield maximum volume of biogas [17].

Several authors have reported on the generation of biogas through food waste [4,5], pineapple waste [8], pharmaceutical wastewater [9],agricultural waste [13]. However, despite its abundance, few reports have considered the use of plantain peel substrate for biogas production. Furthermore, to the best of our knowledge, no work has been reported on the modeling and optimization of the treatment process, which plays a very important role in the modification of the substrates for enhanced biogas generation. Hence, the need for this study.

Pretreatment conditions can be modeled and optimized to increase the amount of biogas produced and bring about the use of minimal energy with low costs [15]. The response surface method (RSM), artificial neural network (ANN), and adaptive neuro-fuzzy inference system (ANFIS) are some advanced modeling tools applied in evaluating the interaction of the different parameters of a process study [18]. RSM generates a mathematical model for evaluating the optimum conditions of a process with minimum number of experiments [19–21]. ANN applies the principles of biological neurons in modeling complex multi-variant processes [22–24], while ANFIS combines neural and fuzzy systems in simulating different industrial processes with a minimum steady error [25,26].

Therefore, in the present study, we intend to (1) harness the effectiveness of artificial intelligence algorithms (ANN and ANFIS) in modeling the pretreatment process of plantain peel substrate for enhanced anaerobic methanogenesis; (2) Study the chemical and morphological implications of the pretreatment process using Fourier transform infrared spectroscopy (FTIR) and scanning electron microscopy (SEM); (3) Investigate the Biogas production kinetics using five exploratory models; (4) Upgrade the produced biogas for biomethane beneficiation. Finally, the obtained residual anaerobic sludge will be characterized for potential agro applications.

2. Materials and methods

2.1. Sourcing and characterization of materials

Unripe plantain peels used for the study were gathered from eateries in Awka, Anambra state, Nigeria. The peels were washed, dried in the sun (average temperature of 33 °C) and pulverized. Proximate analyses were carried out before and after substrate pretreatment using AOAC technique [27]. Instrumental analyses via Scanning electron microscopy (SEM) and Fourier transform infrared (FTIR) analyses were used to determine the substrate's properties before and after pretreatment. Anaerobic digestion was carried out after pretreatment modeling.

2.2. Thermo-chemical pretreatment process

The substrate was subjected to thermo-chemical pretreatment technique to improve the biogas production during the anaerobic digestion process. Caustic soda (NaOH) was used for the pre-treatment process. Effects of NaOH concentration (from 0.10 to 0.20 N), time (20–70 min) and temperature (90–160 °C) of the pretreatment process were investigated [8,28]. These factors were optimized for maximum production of biogas. Different samples of 50 mL NaOH concentrations were mixed with 300 g each of the substrate. The homogeneous distribution of the samples in the solutions was ensured by thorough mixing in a magnetic stirrer (Model: 78HW-1). These mixtures were placed in a Memmet oven at predetermined temperature and time (see Table 3). After pre-treatment, the substrates were washed severely under running water onto pH of 7.

2.3. Anaerobic digestion process

The procedure for anaerobic digestion was carried out using eight anaerobic batch digesters of 1-L volume capacity. Each batch digester was linked by downward displacement to a measuring cylinder held by a retort stand to gauge the amount of biogas (methane) generated by the digester. The digester was charged with the mixture of 200 g of pretreated plantain peel and 400 mL of distilled water. There was no addition of an inoculum. The homogeneity of the contents in the digesters was maintained by stirring the contents thoroughly with a stirrer before securing the seal with rubber cap to maintain airtight and mesophilic conditions. The biogas production process was carried out for 15 days, and the daily biogas yield was recorded as the difference between the initial and final reading for the day. The biogas produced in each digester was collected to determine its composition at the end of the process. The anaerobic sludge generated at the end of the digestion process was also characterized [29].

2.4. Pretreatment modeling with response surface methodology (RSM)

RSM was utilized to design the experiment, carry out multiple regression analysis and solve the multivariate equations simultaneously [30,31].

Three pre-treatment independent variables were used as the input process parameters used inCCD and simulation of the amount of biogas product. The input process variables were the concentration of NaOH (N), temperature (^{o}C), and contact time (mins) while the yield of biogas measured in volume (mL) was the response or output.

As a five-level experimental design, RSM-CCD comprises one level in the center (0), two axial levels (+α and –α) and two factorial levels (+1 and −1) [32,33]. The five-factor level of the process parameters and their values can be determined by consulting the Supplementary Material (ST1).

The performance of the anaerobic process was determined by calculating the responses (Y) as a function of the input process parameters x_1, x_2 … x_k. The relationship was described by Prakash et al. [34] in equation (1).

$$Y = f(x_1, x_2, \ldots x_k) + e \quad (1)$$

where f is the real response function, x_1,x_2, ….$x_k$are the independent process variables, e is the term of error, while k represents the number of independent variables.

The biogas yield was modeled using a second-order polynomial equation. A quadratic equation given in equation (2), was utilized

in evaluating the relevant model terms.

$$Y = \beta_o + \sum_{i=1}^{k} \beta_i X_i ..... + ... \sum_{i=1}^{k} \beta_{ii} X_i^2 ..... + ... \sum_{i=1}^{k-1} \sum_{j=1}^{k} \beta_{ij} X_i X_j \quad (2)$$

where Y is the response (biogas volume); X_i and X_j are independent process variables; $\beta_o$is the model intercept, β_i, β_i, and β_j are model interactive coefficients for linear, quadratic coefficient, and interaction terms; k is the number of independent process factor (k = 3 in this study).

Multiple regressions were used to analyze the experimental data while the weight of each coefficient was assessed using the Fishers test (F-test). The significance of each model term was evaluated by Analysis of variance (ANOVA) while the adequacy of the models was checked using correlation coefficient.

2.5. Artificial neural network-based pretreatment modeling (ANN)

ANN as a computational technique was also used to model the nonlinear relationship between the substrate treatment variables and the biogas yield [34]. ANN is made up of synchronous processing elements inspired by biological neurons. The synchronizing ability of the multi-layered perceptron (MLP) of the ANN was selected in the training and modeling of the biogas production. Back-propagation (BP) algorithm was employed in the predictive modeling with the three variables (NaOH concentration, time, and temperature) serving as inputs to the input layer. The output layer consists of a single node representing the biogas yield. The number of neurons in the hidden layer was determined using trial and error based on both the least mean square error and the highest correlation coefficient. Hence, the topology of the ANN architecture was designated as 3-h-1 (see supplementary material). The number of neurons in the hidden layer was varied between 3 and 15.

Sigmond transfer function used in modeling the hidden layer was given in Eq. (3).

$$f(x) = \frac{1}{1 + \exp^{(-x)}} \quad (3)$$

for which $f(x) = x$.

The neural toolbox of MATLAB 2015 (The Mathworks Inc.) was used for the training, modeling and analysis of the ANN.

2.6. Pretreatment modeling with adaptive neuro-fuzzy inference system (ANFIS)

ANFIS is a hybrid of fuzzy network and neural network maximizing the advantages of both systems. The data sets used in ANN were identical to those used in ANFIS analysis. The IF-THEN rule was used to simulate the ANFIS anaerobic digestion process [35]. It was expressed in equations (4) and (5).

Rule 1: IF A is E_1, B is F_1 and C is G_1,

$$\text{then } f_1 = x_1A + y_1B + z_1C + u_2 \quad (4)$$

Rule 2: IF A is E_2, B is F_2 and C is G_2,

$$\text{then } f_2 = x_2A + y_2B + z_2C + u_2 \quad (5)$$

Where A, B and C are the input variables representing temperature, time, and NaOH concentration of the pretreatment process respectively; f_1 and f_2 are the output functions (biogas yield); E_1, F_1, G_1, E_2, F_2 and G_2 are the language indicators; x_1, y_1, z_1, x_2, y_2, z_2, u_1 and u_2 are the output functions' coefficients.

The five neuro-fuzzy layers of the ANFIS model were simulated as a system with direct connections between them [36]. The ANFIS architecture can be obtained in the Supplementary Material (SF2). The first layer functions as a link between the input parameters and the neuro-fuzzy system. For the input parameters, the second layer acts as a membership function. The fuzzy rules governing the system are represented by the third layer with adaptive nodes on the fourth layer. This controls the node functions of the system. The fifth layer functions as an aggregate of all the outgoing nodes of the system cumulating in the overall output of the fuzzy inference system [24]. The Takagi-Sugeno inference system-based fuzzy logic toolbox of MATLAB 2015 (version 8) was used in the ANFIS modeling.

2.7. Comparison of the three models

Comparison and ranking of ANN, RSM, and ANFIS models was done based on the efficiency of anticipating the biogas volume generated in the process of anaerobic digestion. Standard statistical indices applied in previous works were used to compare and rank the models [28,32,33,37–40]. The equations of the statistical indices were given in the Supplementary Material (ST2). They indicated the degree of deviations of the anticipated biogas volume of the models from the actual experimental result. The smaller the error deviations, the more effective and efficient the particular model will be [28,37,38].

2.8. Kinetics of biogas production

To analyze the anaerobic digestion process, five kinetic models were employed. The curve fitting toolbox of MATLAB 2015 was used to fit the experimental data of the cumulative biogas yield on the individual kinetic models. The kinetic models used in the study were shown in Table 1.

2.8.1. Logistic growth model

Logistic growth equation also referred to as linear growth equation is given in Eq. (6). This kinetic equation assumes that the anaerobic biodegradation process occurs in a linear path with respect to biogas yield.

$$y = \frac{a}{1 + bexp(-kt)} \tag{6}$$

where k is the kinetic constant (day^{-1}), a and b are constants, and t is the hydraulic retention time (days).

2.8.2. Logistic model

The sigmoid gradient is shown by the logistic model (Eq. (7)). It is a progression curve that is frequently used for modelling and predictions. By assuming that the rate of generated biogas is proportionate to the quantity of biogas that has already been produced, it basically aids in the prediction of the initial exponential climb and subsequent stabilisation at maximum production rates [42].

$$y = \frac{P}{\left[1 + \exp\left(4R_m \times \frac{\lambda - t}{P} + 2\right)\right]} \tag{7}$$

Where λ is the lag phase, P is the biogas production potential, and the maximum production rate is denoted by R_m.

2.8.3. Modified Gompertz model

A modified Gompertz theory of nonlinear modelling (Eq. (8)) is primarily employed to take into account the lag phase (λ) period, biogas production potential (Bo), and biogas production rate (μ_m).

$$y = Bo.exp\left\{ - exp\left[\frac{\mu_m.e}{Bo}(\lambda - t) + 1\right]\right\} \tag{8}$$

This model is also utilized when inhibition of the AD process becomes apparent with the assumption that biogas generation indicates growth of bacteria [43,45].

A plot of cumulative biogas yield against time is used to estimate the kinetic constants.

2.8.4. Multi-stage processes

For determining the cumulative biogas output, particularly in multiple-stage processes, some authors have extensively revised the Modified Gompertz solution [45,46]. These modifications the modified superimposed model (Eq. (9)), and *trans*-Gompertz model (Eq. (10)) which were applied in this work to test for multi-stage anaerobic digestion processes.

2.8.4.1. Modified superimposed model. The superimposed model, which essentially proposes that two phases occur through the breakdown of specific feedstocks, was created by fusing first order kinetic model with the modified Gompertz model. The fast use of readily biodegradable substrates is associated with the first phase, while the unfavourably biodegradable substrates are associated with the second phase [47,46]. The modified superimposed model which is a derivative of the superimposed model was formed by combining a modified form of the first order model and the modified Gompertz model as given in Eq. (9).

$$y = G_{01}[0.45\ -\exp(-\mathrm{kt})] + G_{02}.exp\left\{ - exp\left[\frac{\mu_m.e}{G_{02}}(\lambda - t) + 1\right]\right\} \tag{9}$$

Table 1
Summary of Kinetic Models applied in the anaerobic digestion.

Kinetic model	Equation	Eq. No	Ref.
Logistic growth	$y = \frac{a}{1 + bexp(-kt)}$	(6)	[41]
Logistic	$y = \frac{P}{\left[1 + \exp\left(4R_m \times \frac{\lambda - t}{P} + 2\right)\right]}$	(7)	[42]
Modified Gompertz	$y = P.exp\{ - exp[\frac{\mu_m.e}{P}(\lambda - t) + 1]\}$	(8)	[43]
Modified superimposed model	$G_{01}[0.45\ -\exp(-\mathrm{kt})] + G_{02}.exp\left\{ - exp\left[\frac{\mu_m.e}{G_{02}}(\lambda - t) + 1\right]\right\}$	(9)	[44]
Trans-Gompertz model	$B_{01}\left\{1 - \exp\left[\frac{-R_m(t - \lambda)}{G_{01}}\right]\right\} + B_{02}.exp\left\{ - exp\left[\frac{\mu_m.e}{B_{02}}(\lambda - t) + 1\right]\right\}$	(10)	[44]

where G_{01}: represents the optimum specific methane output from substrates that degrade rapidly (mL/g VS); G_{02}: represents the specific methane yield (mL/g VS) from feedstock with weak biodegradability (mL/g VS). k: Constant rate of biogas or produced methane.

2.8.4.2. Trans-Gompertz model. Trans-Gompertz model was developed by coupling the Transfer function model and the modified Gompertz model. Transfer function model is developed from first order kinetic model by replacing the kinetic constant (k) for the proportion of the maximal biogas production scale (R_m) to the substrate's biogas capacity (B_{o1}) [44]. The *trans*-Gompertz model used in the work is given in Eq. (10).

$$y = B_{01}\left\{1 - \exp\left[\frac{-R_m(t-\lambda)}{G_{01}}\right]\right\} + B_{02}.exp\left\{-exp\left[\frac{\mu_m.e}{B_{02}}(\lambda - t)+1\right]\right\} \quad (10)$$

where B_{01}: represents the optimum specific methane output from substrates that degrade rapidly (mL/g VS); B_{02}: represents the specific methane yield (mL/g VS) from feedstock with weak biodegradability (mL/g VS). k: Constant rate of biogas or produced methane. $R_m and \mu_m$ are the maximum biogas production rate in the first and second phase, respectively.Where R_m, μ_m = Maximum biogas production rate, ml/day; B_{max}, P = Biogas production potential, ml; y = Predicted cumulative biogas volume, ml; t = HRT, day; k = rate constant, day^{-1}; λ = lag phase, day; exp = Euler's constant = exp(1) = 2.7183; a, b = constants [8,47].

2.9. Biogas analysis and purification

The raw and purified biogas was analyzed using Horib Gas Analyzer (model number: PG-433). This was used to determine the composition of the biogas before and after scrubbing. In order to purify and enhance the methane content, it was scrubbed using sodium hydroxide and activated charcoal.

An overall flowchart of methodology implemented in the present study was presented in the supplementary material.

3. Results and discussion

3.1. Proximate analysis of the substrate

The result of proximate analysis of the substrate before digestion was shown in Table 2. The pH of the substrate was 6.65 which was comparable to the 6.4 and 6.7 obtained for plantain peel by Ilori *et al.* [48] and Abubakar [49], respectively. It is important to note that pH less than 8.5 is suitable for methanogenic bacteria. The presence of N, P, and K indicate that the substrate can be a source of fertilizer [50]. The C/N ratio showed that the substrate can be used as a soil conditioner with enhanced flow properties and accelerated soil absorption of the digestate. C/N ratio has been reported to significantly influence biogas production factors such as biodigestion time, and biogas yield. According to Dai et al., increase in C/N ratio prolonged the biodigestion time of substrates which is attributable to high carbon content.

3.2. Instrumental analysis of the substrate

3.2.1. Fourier transform infrared (FTIR) analysis

The FTIR analysis was used to ascertain the major functional groups in the yam peel substrate. The spectra of untreated and treated plantain peel substrates were compared in Fig. 1 (a) and 1 (b), respectively. The changes in the spectrum of the treated substrate and the wave numbers showed that structural modifications took place in the substrate after the treatment. More peaks were detected after the substrate treatment which revealed the presence of some compounds such as esters, alkenes, ethers, carboxylic acids etc. This may be because of the elimination of associated bond matters and lignin following substrate treatment process [51]. The bandwidth at 3276.3 cm^{-1} was linked with the level of inter-molecular and intra-molecular hydrogen bonding. The peaks at 1420 cm^{-1} and 1319 cm^{-1} with shoulder bands were due to aliphatic CH_2 and symmetric/asymmetric CH_3, respectively. The observed modifications in the

Table 2
Proximate analysis of the substrate.

Parameter	Numerical value
Moisture content (%)	51.52 ± 1.20
Nitrogen content (N, %)	2.43 ± 0.50
Total suspended solids (TSS, mg/l)	55.05 ± 0.001
Total volatile solids (TVS, %)	28.06 ± 0.05
Carbon content (%)	41.83 ± 1.96
C/N Ratio	17.21 ± 1.14
pH	6.65 ± 0.45
Phosphorus (P, %)	1.02 ± 0.17
Potassium (K, %)	1.08 ± 0.19
Ash content (%)	9.75 ± 1.06

Table 3
Experimental biogas yield and models' predictions.

Exp. run	Temp. (°C)	Time (mins)	Conc. (N)	Exp. Biogas yield (mL/gVS)	Models' predicted biogas yield (mL/gVS)			Residuals		
					RSM	ANN	ANFIS	RSM	ANN	ANFIS
1	100	60	0.15	175	167.56	174.83	174.66	7.44	0.17	0.33
2	100	30	0.15	219	213.23	219.71	219.66	5.77	−0.72	−0.66
3	89.7	45	0.125	161	175.46	160.57	160.66	−14.46	0.427	0.33
4	160.3	45	0.125	150	129.66	150.00	150.00	20.34	−0.002	0.00
5	125	45	0.125	178	188.84	188.35	186.75	−10.84	−10.35	−8.75
6	100	30	0.1	181	175.13	180.37	180.33	5.87	0.625	0.67
7	125	45	0.160	170	172.76	170.00	170.00	−2.76	−0.003	0.00
8	100	60	0.1	105	104.46	104.85	105.00	0.54	0.145	0.00
9	150	60	0.1	160	169.2	159.86	160.00	−9.2	0.141	0.00
10	125	45	0.160	170	172.76	170.00	170.00	−2.76	−0.003	0.00
11	125	45	0.125	176	188.84	188.35	186.75	−12.84	−12.35	−10.8
12	160.3	45	0.125	150	129.66	150.00	150.00	20.34	−0.002	0.00
13	160.3	45	0.125	150	129.66	150.00	150.00	20.34	−0.002	0.00
14	125	66.2	0.125	150	144.07	149.83	149.66	5.93	0.167	0.333
15	100	30	0.1	180	175.13	180.37	180.33	4.87	−0.375	−0.33
16	125	45	0.089	191	182.03	190.59	190.33	8.97	0.408	0.67
17	125	45	0.125	196	188.84	188.35	186.75	7.16	7.645	9.25
18	100	60	0.1	106	104.46	104.85	105.00	1.54	1.145	1.00
19	100	30	0.15	220	213.23	219.72	219.66	6.77	0.281	0.33
20	150	30	0.1	149	159.87	150.20	150.00	−10.87	−1.197	−1.00
21	150	30	0.15	80	83.63	80.340	80.33	−3.63	−0.342	−0.33
22	100	60	0.1	104	104.46	104.85	105.00	−0.46	−0.854	−1.00
23	125	23.8	0.125	170	169.72	169.49	169.66	0.28	0.508	0.33
24	150	30	0.1	151	159.87	150.20	150.00	−8.87	0.802	1.00
25	125	45	0.125	176	188.84	188.35	186.75	−12.84	−12.35	−10.75
26	125	23.8	0.125	169	169.72	169.49	169.66	−0.72	−0.491	−0.66
27	125	45	0.125	176	188.84	188.35	186.75	−12.84	−12.35	−10.75
28	150	60	0.15	111	117.96	110.12	110.00	−6.96	0.831	1.00
29	89.7	45	0.125	161	175.46	160.57	160.66	−14.46	0.427	0.33
30	125	45	0.160	170	172.76	170.00	170.00	−2.76	−0.003	0.00
31	125	45	0.125	197	188.84	188.35	186.75	8.16	8.645	10.25
32	100	60	0.15	174	167.56	174.83	174.66	6.44	−0.833	−0.66
33	125	45	0.089	191	182.03	190.59	190.33	8.97	0.4082	0.666
34	125	23.8	0.125	170	169.72	169.49	169.66	0.28	0.5084	0.333
35	100	30	0.1	180	175.13	180.37	180.33	4.87	−0.375	−0.333
36	150	60	0.1	159	169.2	159.86	160.00	−10.2	−0.860	−1.00
37	150	60	0.15	109	117.96	110.17	110.00	−8.96	−1.169	−1.00
38	100	30	0.15	220	213.23	219.72	219.66	6.77	0.2807	0.333
39	100	60	0.15	175	167.56	174.83	174.66	7.44	0.1665	0.333
40	125	45	0.125	197	188.84	188.35	186.75	8.16	8.6448	10.25
41	125	45	0.089	189	182.03	190.59	190.33	6.97	−1.592	−1.333
42	150	60	0.1	161	169.2	159.86	160.00	−8.2	1.1411	1.00
43	89.7	45	0.125	160	175.46	160.57	160.66	−15.46	−0.572	−0.66
44	150	60	0.15	110	117.96	110.17	110.00	−7.96	−0.169	0.00
45	150	30	0.15	81	83.63	80.34	80.333	−2.63	0.6576	0.666
46	125	66.2	0.125	149	144.07	149.83	149.66	4.93	−0.833	−0.666
47	125	66.2	0.125	150	144.07	149.83	149.66	5.93	0.1668	0.333
48	150	30	0.1	150	159.87	150.20	150.00	−9.87	−0.197	0.00
49	150	30	0.15	80	83.63	80.34	80.33	−3.63	−0.342	−0.33
50	125	45	0.125	198	188.84	188.35	186.75	9.16	9.645	11.25

spectrum of the treated substrate at 3276.3 cm^{-1} and 2922.2 cm^{-1} wavelengths corresponded to H–*O*–H stretching of the carboxylic acid. Wave numbers in the region of 2100–2200 cm^{-1} represent C–*O*–C stretching of esters. These results correlate with the observations of Iheanacho et al. [52].

3.2.2. Scanning electron microscopy (SEM)

Fig. 2 (a) and 2 (b) show a comparison of the results of scanning electron microscopy for untreated and a pretreated substrate. It displayed the substrate's surface morphology at 1500× magnification. The results show that themacropores were more visible after the substrate treatment. It was also observed that the untreated substrate contained more compact and cemented particles, with a flat, rigid, and smooth surface. The morphology of the untreated substrate revealed densely packed and non-distinctive surface cavities. However, the pretreated substrate showed the presence of large loosely packed pores on the surface of the substrates and the solubilization of the substrate. This may be due to the elimination of bonding materials during the treatment process. This is an indication that pretreatment using the thermo-chemical method altered the structure of the substrate with the degradation of carbohydrate,

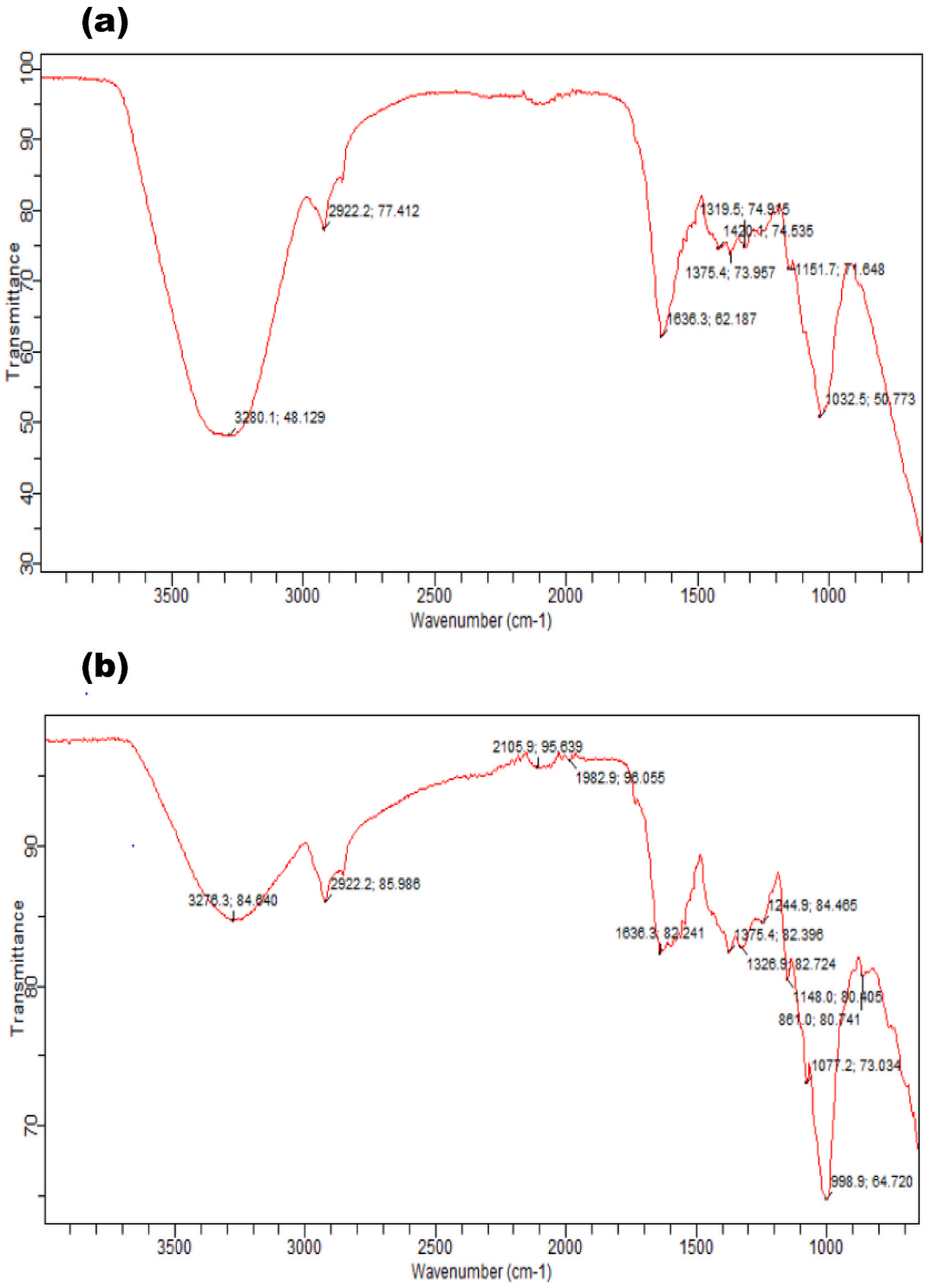

Fig. 1. FTIR result for (a) untreated substrate and (b) treated substrate.

protein, and fat which definitely led to an increase in the biogas production. A similar result was reported by Bala et al. [53].

3.3. RSM modeling of the pretreatment process

The result of the experimental design and the models' predictions was presented in Table 3. The produced biogas volume ranged

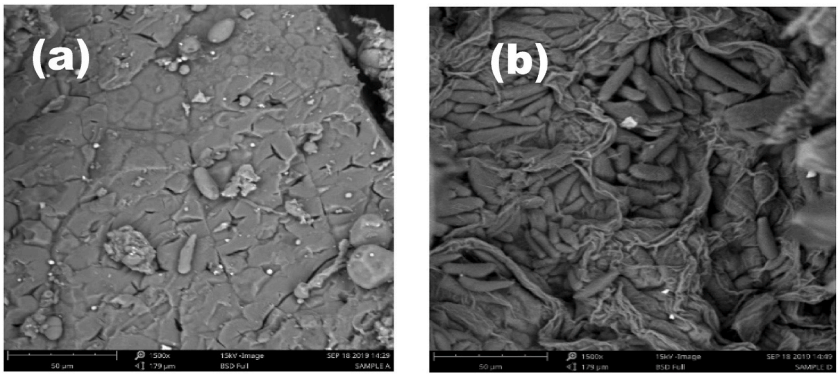

Fig. 2. SEM images of the (a) untreated substrate and (b) treated substrate.

from 80 to 220 mL/gVS. Power transformation will have a negligible effect since the ratio of maximum to minimum response (2.7) was less than 3.0. The process parameters were significantly different, indicating that they had an impact on the biogas yield.

The results of RSM modeling using the experimental data on the linear, two-factor interaction (2FI), and quadratic models were given in the Supplementary Material (ST3). The parameters used to determine the most appropriate model were high correlation coefficient and low standard deviation. The most suitable model for simulating the volume of biogas generated using the specified input variables was the quadratic model. It had a correlation coefficient of 0.9281 with a standard deviation of 10.30. This suggested that the quadratic model can predict experimental data with an accurately of 92.81 %.

A second order polynomial model given in equation (11) was generated and used to express the relationship between the cumulative volume of biogas and the input variables. The model can be used to predict the biogas volume for any given level of input parameters.

$$\text{Biogas yield} = 188.84 - 16.22*A - 9.09*B - 3.28*C + 20*A*B - 28.58*A*C + 6.25*B*C - 18.2*A\text{^}2 - 16.02*B\text{^}2 - 5.74*C\text{^}2 \quad (11)$$

The summary of analysis of variance (ANOVA) of the quadratic model was presented in Table 4. Analysis of variance studies the statistical significance of the second-order model and the corresponding model terms. The acceptability of the model and the model terms were determined using the Fishers value (F-value) and p-value at 95 % confidence level. Model terms with p-values less than 0.05 were selected to be significant [18,54]. A higher F-value and a smaller p-value were desired for accurate modeling. The p-value checks the importance of the coefficients which aids to understand the mutual interactions of the variables [55,56].

For the quadratic model, the F-value and p-value of 57.39 and < 0.0001 respectively indicated that the adopted quadratic model was very significant. The only non-significant term, according to the p-values in the ANOVA Table, was NaOH conc. (C). The insignificant term can be eliminated to give the final model in Eq. (12).

$$\text{Biogas yield} = 188.84 - 16.22*A - 9.09*B + 20*A*B - 28.58*A*C + 6.25*B*C - 18.2*A\text{^}2 - 16.02*B\text{^}2 - 5.74*C\text{^}2 \quad (12)$$

Predicted sum of squares (PRESS) of 6442.05 showed that the model can be used to navigate design space while also validating the reliability of the model. The coefficient of variance (CV) was 6.43 % while the adequate precision ratio (APR) was 28.14. The CV measured the reproducibility of the quadratic model. According to Onu et al. [57], a CV of less than 10 % ensures effective

Table 4
ANOVA of the quadratic process.

Source	Sum of Squares	df	Mean Square	F-Value	p-value
Model	54785.67	9	6087.3	57.39	<0.0001
A-Temperature	9457.18	1	9457.18	89.16	<0.0001
B-Time	2968.26	1	2968.26	27.98	<0.0001
C–NaOH Concentration	388.05	1	388.05	3.66	0.0630
AB	9600	1	9600	90.51	<0.0001
AC	19608.17	1	19608.17	184.86	<0.0001
BC	937.5	1	937.5	8.84	0.0050
A^2	7164.52	1	7164.52	67.54	<0.0001
B^2	5555.21	1	5555.21	52.37	<0.0001
C^2	713.11	1	713.11	6.72	0.0132
Residual	4242.83	40	106.07		
Lack of Fit	3381.99	5	676.4	27.5	<0.5831
Pure Error	860.83	35	24.6		
Cor Total	59028.5	49			
CV	6.43				
Adeq. precision	28.14				

reproducibility of the experimental data. APR evaluated the signal-to-noise ratio. APR values greater than 4 suggest sufficient signal and adequate model efficacy [58]. APR of 28.14 confirmed adequate model signal in predicting the biogas volume. The adjusted R^2 of 0.9119 was in close agreement to the predicted R^2 of 0.8909.

3.3.1. Diagnostic plots

Graphical estimations involving perturbation plot and residuals vs run plot were also used to study the characteristics of the volume of biogas yield and the residual (the difference between the predicted and experimental values). The perturbation and the residual vs run showed deviation from the reference point which is the mean and the magnitude of error encountered in each experimental run respectively (see supplementary material). NaOH Concentration showed the least deviation from the mean as the reference point ranged from −1 to +1. The highest positive and negative deviations were observed in experiments 4 and 10 respectively. Most of the residuals were of negligible values confirming the suitability of the quadratic model.

3.4. ANN modeling of pretreatment process

The experimental dataset was divided into seventy percent, fifteen percent and fifteen percent for training, testing, and validation respectively. The correlation between the output and input parameters was established by the training data set. The validation and testing datasets evaluated the neural network generalization and neural network prediction accuracy, respectively [24].

Different numbers of neurons in the hidden layer ranging from 5 to 15 were tested for optimum performance of the network using mean square error (MSE) index. Ten neurons in the hidden layer gave the optimum performance with the minimum MSE as shown in Fig. 3. Therefore, the neural network was created using 10 neurons. The optimal neural architecture was 3-10-1 representing three input neurons for the three input parameters, ten neurons in the hidden layer, and a single output neuron for the biogas volume.

The architecture used in the modeling of ANN was the sigmoidal function multi-layer perceptron (MLP). The performance plot was used to evaluate the reliability of the neural validation of the network training process for 5 epoch iterations. The testing curve did not suggest any significant increase over the validating curve. The three curves stabilized at the 3rd epoch. There was no over-fitting problem with the network since an insignificance MSE of 2.83×10^{-4} was obtained at the 4thepoch iteration. This result validated to the reliability of the neural network in predicting the biogas volume produced through anaerobic digestion of the present system. Properties of the ANN model was presented in Table 5 together with those of the ANFIS model.

ANN regression plots were shown in Fig. 4. Correlation coefficients of the training (Fig. 4 (a)), validation (Fig. 4 (b)), and testing (Fig. 4 (c)) data sets were 0.9951, 0.9936, and 0.9526 respectively while the MSE were 0.000277, 0.000283, and 0.000843 respectively. These values proved that both the network response and the ANN topology chosen were acceptable. Correlation coefficient of the overall data set (Fig. 4 (d)) was 0.9991 demonstrating that the anaerobic digestion's output followed its aim in a satisfactory manner [59].

3.5. ANFIS modeling of pretreatment process

The membership function used was Gaussian membership function (gaussmf) and the FIS generation employed was Grid partition with linear output function. In order to create the fuzzy inference system, three membership functions (MFs) were assigned to each of the input layers. The input data was initiated as a 150×3 matrix into the MATLAB m-file while the output data was a single column matrix of 150 datasets. Like in the ANN modeling, the data sets were divided into testing, training, and checking data sets. The R^2 obtained for the training, testing, and checking were 0.9861, 0.9909, and 0.9725 while the MSE values were 0.0189, 0.0152, and 0.0205 respectively. These desirable values showed adequate ANFIS modeling.

The overall ANFIS training with 30 designated epoch iterations was illustrated in Fig. 5 (a). The training was finished at epoch 19 with mean square error was 0.01886 with 27 linear parameters and 18 non-linear parameters. The training curve became approximately constant at epoch 17 with 27 fuzzy rules. The low MSE demonstrated that ANFIS technique was effective in modeling the present system [26]. The ANFIS predicted biogas yields for the initial experimental dataset were given in Table 3. In terms of the anaerobic digestion process, the ANFIS correlation coefficient was 0.9852 which proved the adequacy of the model. The tracking of

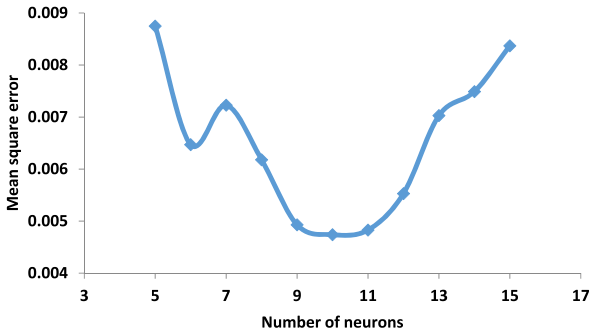

Fig. 3. Plot of number of neurons against mean square error.

Table 5
Properties of the ANN and ANFIS models.

ANN model		ANFIS model	
Algorithm	Back propagation	Number of inputs	3
Training function	Levenberg-Marquardt	Number of MF for each input	3
Error function	Mean square error	Number of outputs	1
Input layer neurons	3	Number of epochs	30
Output layer neurons	1	FIS	Sugeno
Hidden layer neurons	10	Number of training data pairs	150
Hidden layer	fitnet	Input MF	Trimf
Training network	trainlm	Output MF	Constant
Epoch iterations	5	Number of fuzzy rules	27
Data division	dividerand	Number of nodes	78

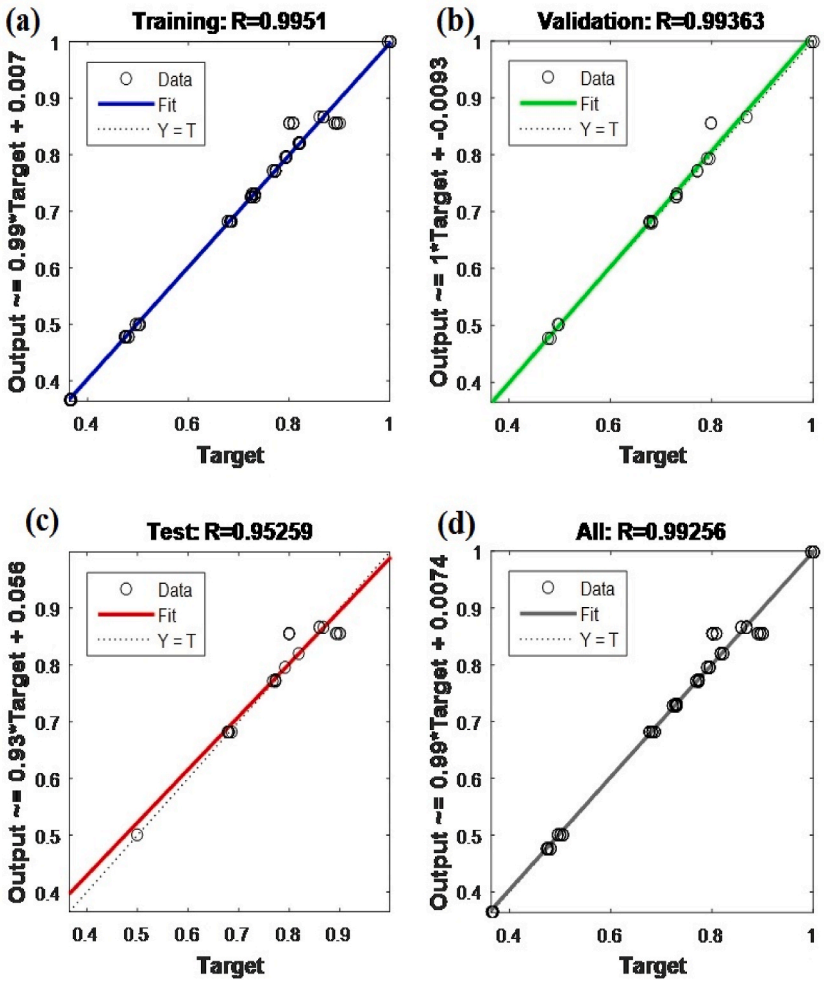

Fig. 4. Correlation coefficient for ANN network performance for (a) Training data, (b) Validation data, (c) Testing data, and (d) All data.

each experimental datawith each FIS predicted volume of biogas yield is presented in Fig. 5b.

3.6. Comparative assessment of the models

The result of statistical analysis of the three models was presented in Table 6. The comparative assessment of the three models was based on the statistical indices highlighted in Table 6.

The results showed that the R^2 of the three models were all greater than the reported 0.8 needed for a significant correlation between predicted response and experimental response [60]. To rank the models, other statistical terms such as ARE, HYBRID, RMSE,

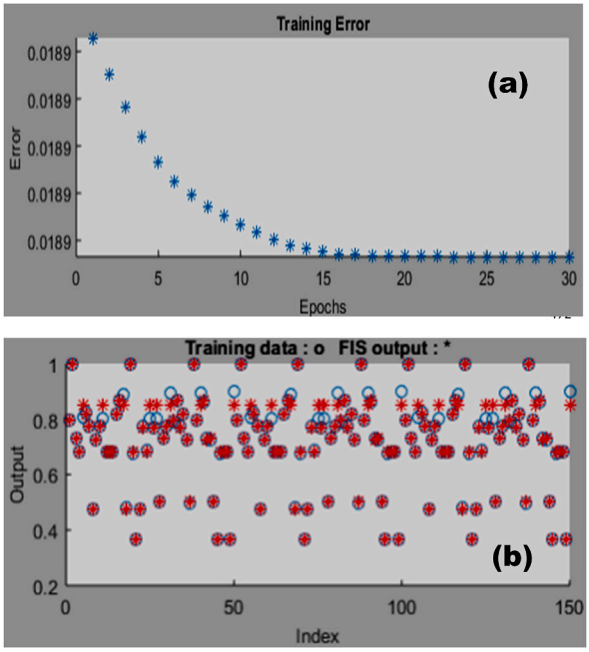

Fig. 5. ANFIS (a) training error plot and (b) distribution of predicted with experimental outputs.

Table 6
Models' statistical analysis.

Statistical term	RSM	ANN	ANFIS
SSE	1113.34	48.157	26.83
HYBRID	18.556	0.803	0.447
ARE	3.6088	0.6984	0.2791
RMSE	0.04799	0.00969	0.00587
R^2	0.9281	0.9850	0.9852
Adj R^2	0.9119	0.9844	0.9846

and SSE were evaluated between the experimental values and predicted values. The ANFIS model was found to be more efficient than the ANN model with lower values of the error terms. RSM model though effective, was comparatively the least among the three models. This trend is in agreement with the reports of Onu et al. [57], Betiku et al. [60], and Karimi et al. [61]. Hence, ANFIS was found to be the best modeling technique followed by ANN and RSM models, in the production of biogas from the anaerobic digestion of plantain peel substrate.

3.7. Interactive effects of the process variables

The interactive effect between two process variables was studied with the aid of the 2D contour plots as shown in Fig. 6 (a), (b) and (c).

Two input variables were varied within the experimental range with the third variable held constant. The relationship between time and temperature indicated that an increase in both variables resulted to increase in the biogas yield though temperature had a bigger effect on the biogas production. The p-value of all the interactive effects was less than 0.0001 showing that not just the individual effects but also the combined effect of any two variables has a substantial impact on the volume of biogas produced [26]. An optimum biogas yield of 200.104 mL was obtained at a temperature of 102.67 °C and time of 31.68 min with NaOH concentration set at null point (Fig. 6a) while 205.446 mL and 191.296 mL were obtained with time and temperature set at null points respectively (Fig. 6b and c).

3.8. Optimization of digestion process

The goal was the minimization of temperature and the maximization of the biogas yield. The time and the NaOH concentration were set within the experimental range. An optimum biogas yield of 215.35 mL was obtained at temperature, time, and NaOH concentration of 100 °C, 35.96 min, and 0.150 N, respectively. The optimum biogas production was validated using the test-retest method and an average of 217.0 mL was obtained.

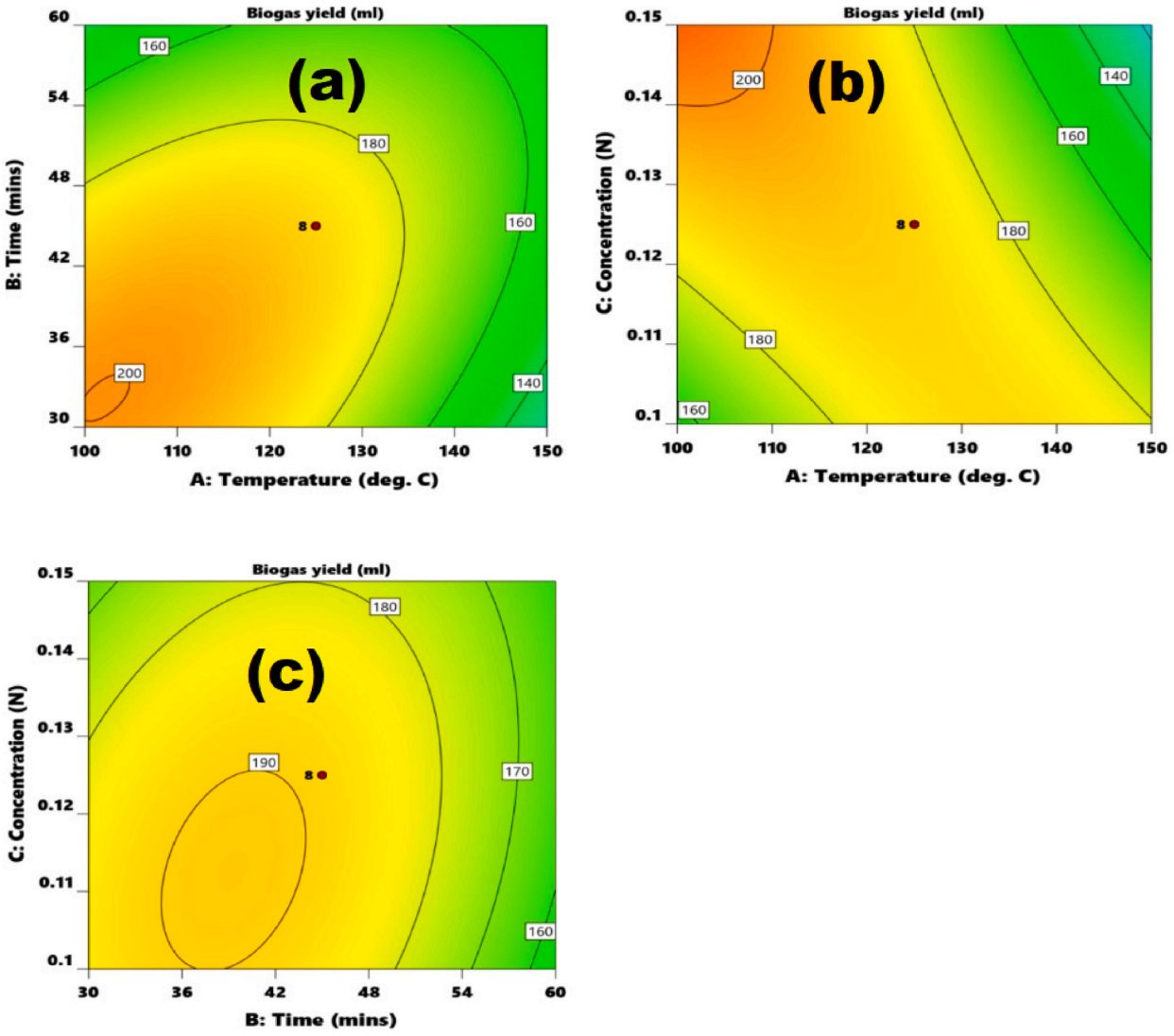

Fig. 6. 3D contour plots depicting interactions between (a) temperature and time, (b) temperature and NaOH concentration and (c) time and NaOH concentration.

The significance of each of the process parameter was investigated through the experimental model in percentage. The significance of temperature, time and NaOH concentration were 74.09, 23.04 and 2.88 % respectively. This implied that temperature of the treatment process had the most significant effect while concentration of NaOH has the least effect on the substrate treatment.

3.9. Kinetics of the anaerobic process

Five non-linear kinetic models were used: Logistic, Modified Gompertz, Transference, Exponential rise to maxima, and Modified Logistics models. The experimental cumulative biogas yield was fitted into the equation of these models and the correlation coefficient, models' constants, and statistical error functions were evaluated and presented in Table 7. The experimental curve (see Fig. 7) indicated that the first three days resulted in no biogas yield. This stage is regarded as the hydrolysis stage where the complex organic substances are split into simpler substances needed for the acid-genesis fermentation stage [62,63]. Then a steep increase in the biogas yield was observed before it stabilized at a constant value. The kinetic analysis showed that the most suitable model describing the total biogas production was by the Logistic model, followed by the Modified Logistics with correlation coefficients of 0.9912 and 0.9904 and root mean square error of 0.4772 and 0.4861 respectively. Since the Logistics model best matched the anaerobic digestion's kinetics, the exponential phase followed first-order kinetics [62] and the mechanism of the reaction was auto-catalytic [64]. Transference model with correlation coefficient of 0.9379 was equally adept in explaining the kinetics of the process.

Table 7
Result of anaerobic digestion kinetic modeling.

Kinetic parameters	Parametric Values
Logistic growth model	
a	242.8
b	1070
K	−1.195
SSE	1524
R^2	0.9906
Adj R^2	0.989
RMSE	11.27
Logistic model	
λ	4.164
P	242.8
R_m	72.52
SSE	1524
R^2	0.9906
Adj R^2	0.989
RMSE	11.27
Modified Superimposed model	
G_{o1}	5.78
G_{o2}	246.2
λ	4.034
μ_m	20.06
k	0.08029
e	9.699
SSE	631.9
R^2	0.9961
Adj R^2	0.9939
RMSE	8.379
Modified Gompertz Model	
Bo	246.6
e	13.53
μ_m	14.14
λ	4.06
SSE	651.3
R^2	0.996
Adj R^2	0.9949
RMSE	7.695
Trans-Gompertz model	
B_{o1}	204.3
R_m	2.011
λ	4.11
B_{o2}	229.8
μ_m	23.69
e	8.468
SSE	527.4
R^2	0.9967
Adj R^2	0.9949
RMSE	7.655

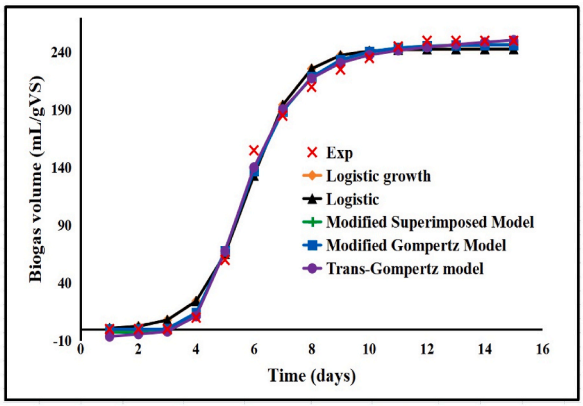

Fig. 7. Kinetic modeling of the anaerobic digestion process.

3.10. Biogas purification and analysis

Major composition of the biogas before and after purification was presented in Table 8. The biogas consisted of methane which is the main component of biogas, and carbon IV oxide in addition to small traces of hydrogen sulphide, water vapour, nitrogen, ethanol, etc. The purification process was used to increase the energy per unit volume of the biogas by eliminating hydrogen sulphide and carbon IV oxide. The hydrogen sulphide is responsible for corrosivity and toxicity while carbon IV oxide decreases both the biogas quality and the heating value [65,66]. The percentage of methane in the purified gas increased to about 94 % while carbon IV oxide and hydrogen sulphide decreased considerably.

3.11. Characteristics of the anaerobic sludge

The characterization of the sludge after digestion was shown in Table 9. The C/N ratio of the waste sludge was observed to reduce at the end of digestion. This was because the microorganisms in the substrates had insufficient carbon and nitrogen source with such low C/N ratio indicating its potential applicability in enhancement of agricultural processes [59], [67]. The TSS and TVS reduced after the anaerobic digestion when compared with the initial characterization in Table 1. This was due to gradual fermentation of the organic solids by microbes for the acidogenesis stage. For anaerobic digestion, the values of TSS and TVS decreased as the hydraulic retention time increased slowing down at the end of the anaerobic process [68,69]. The increase in the values of the N, P, and K after digestion indicated that the slurries could be used as fertilizer [50].

4. Conclusion

This work centered on the modeling of substrate treatment for enhanced biogas production from waste plantain peel substrate through anaerobic digestion process. Thermo-chemical treatment process variables such as time, NaOH concentration and temperature were modeled using RSM, ANN, and ANFIS. The instrumental analysis via FTIR and SEM showed the modification of the functional groups and the structural changes in the morphology of the substrate after the pretreatment. Logistic and Modified Logistic kinetic models were most adequate in describing the anaerobic digestion process. RSM, ANN, and ANFIS were efficient in modeling the thermo-chemical substrate treatment with values of coefficient of correlation as 0.9281, 0.9850, and 0.9852, respectively. Supplementary indices of statistics confirmed that ANFIS model was slightly superior to ANN model in stimulating and predicting the biogas yield. Enhancing the ANFIS model through optimization gave 217.0 mL of biogas per 200 g/400 mL substrate-water mixture at temperature of 102.7 °C, NaOH concentration of 0.125 N and treatment time of 31.7 min. Biogas purification through scrubbing increased the methane composition of the biogas to about 94.0 %. The waste slurry from the anaerobic process could be used as manure in agriculture. The result of this study was therefore recommended for possible industrial biogas production with special emphasis on the initial treatment of the substrates which will increase the anaerobic digestion process's capacity to produce biogas.

Funding

This research did not receive any specific grant from funding agencies in public, commercial or not-for-profit sectors.

Availability of data and materials

The results/data/figures in this manuscript have not been published elsewhere, nor are they under consideration (from Contributing Authors) by another publisher. However, data will be made available on request.

CRediT authorship contribution statement

Chinenyenwa Nkeiruka Nweke: Conceptualization. **Chijioke Elijah Onu:** Methodology, Investigation, Data curation, Conceptualization. **Joseph Tagbo Nwabanne:** Writing – original draft, Visualization, Supervision, Project administration, Conceptualization. **Paschal Enyinnaya Ohale:** Writing – review & editing, Writing – original draft, Validation, Software, Methodology, Formal analysis, Data curation, Conceptualization. **Emeka Michael Madiebo:** Writing – original draft, Software, Investigation, Data curation. **Monday Morgan Chukwu:** Validation, Software, Data curation.

Table 8
Compositions of the biogas.

Components	Before purification (%)	After purification (%)
Methane	51.0	94.0
Carbon dioxide	43.5	3.0
Hydrogen sulphide	2.2	1.3
Water vapour	1.5	1.1
Others	1.8	0.7

Table 9
Characteristics of the anaerobic sludge.

Parameter	Numerical value
TSS (g/Kg)	12.28
VS (%)	5.8
Carbon (C, %)	24.77
Nitrogen (N, %)	2.24
C/N ratio	11.06
Phosphorus (P, %)	0.84
Potassium (K, %)	0.96
pH	4.02
Ash (%)	9.47
Moisture (%)	65.75

Declaration of competing interest

The authors declare that they have no known competing financial interests or personal relationships that could have appeared to influence the work reported in this paper.

Acknowledgment

The authors would like to thank the Chemical Engineering department for providing conducive environment that enabled this research work to be carried out.

Appendix A. Supplementary data

Supplementary data to this article can be found online at https://doi.org/10.1016/j.heliyon.2023.e21995.

References

[1] N. Ferronato, V. Torretta, Waste mismanagement in developing countries: a review of global issue, Int. J. Environ. Res. Publ. Health 16 (2019) 1–28.
[2] C. Ike, C. Ezeibe, S.C. Anijiofor, N.N.N. Daud, Solid waste management in Nigeria: problems, prospects, and policies, J. Solid Waste Technol. Manag. 44 (2) (2018) 163–172, https://doi.org/10.5276/JSWTM.2018.163.
[3] A. Roopnarain, R. Adeleke, Current status, hurdles and future prospects of biogas digestion technology in Africa, Renew. Sustain. Energy Rev. 67 (2017) 1162–1179.
[4] H. Yong, K. Takuro, Z. Guangyin, S. Chen, X. Kai-Qin, Effects of lipid concentration on thermophilic anaerobic co-digestion of food waste and grease waste in a siphon driven self-agitated anaerobic reactor, Bioresour. Technol. Rep. 19 (2018), https://doi.org/10.1016/j.btre.2018.e00269.
[5] K. Faisal, H. Abdullah, N. Muhammad, A. Habibullah, Production of biogas by anaerobic digestion of food waste and process simulation, Am. J. Mech. Eng. 3 (3) (2015) 79–83, https://doi.org/10.12691/ajme-3-3-2.
[6] M. Perea-Moreno, E. Samerón-Manzano, A. Perea-Moreno, Biomass as renewable energy: worldwide research trends, Sustainability 11 (863) (2019) 1–9, https://doi.org/10.3390/su11030863.
[7] G.G. Longjan, Z. Dehouche, Biogas production potential of co-digested food waste and water hyacinth common to the Niger Delta, Biofuels 11 (3) (2020) 277–287, https://doi.org/10.1080/17597269.2017.1358950.
[8] P.E. Ohale, C.E. Onu, M.I. Ejimofor, et al., Development of a Surrogate Model for the Simulation of Anaerobic Co-digestion of Pineapple Peel Waste and Slaughterhouse Wastewater: Appraisal of Experimental and Kinetic Modeling, Environmental advances, 2023, https://doi.org/10.1016/j.envadv.2022.100340.
[9] L.N. Emembolu, J.T. Nwabanne, C.E. Onu, I.O. Obiakor, Simulation of kinetic model for anaerobic digestion of pharmaceutical wastewater, Chem. Sci. Int. J. 20 (3) (2017) 1–13, https://doi.org/10.9734/CSJI/2017/34050.
[10] D. Nguyen, N. Saoharit, S. Chayanon, K.C. Surendra, K.K. Samir, Biogas Production by Anaerobic Digestion: Status and Perspectives. Biofuels: Alternative Feedstocks and Conversion Processes for the Production of Liquid and Gaseous Biofuels, 2019, pp. 763–778, https://doi.org/10.1016/B978-0-12-816856-1.00031-2 (Chapter 31).
[11] U.E. Kiran, K. Stamatelatou, G. Antonopoulou, G. Lyberatos, Production of biogas via anaerobic digestion, Handbook of Biofuels Production 2e (2016) 259–301, https://doi.org/10.1016/B978-0-08-100455-5.00010-2 (Chapter 10).
[12] K. Rajendran, A. Solmaz, J.T. Mohammad, Household biogas digesters—a review, Energies 5 (2012) 2911–2942, https://doi.org/10.3390/en5082911.
[13] A.M. Ziganshin, J. Liebetrau, J. Proter, S. Kleinsteuber, Microbial community structure and dynamics during anaerobic digestion of various agricultural waste materials, Appl. Microbiol. Biotechnol. 97 (2013) 5161–5174.
[14] J. Jamison, S.K. Khanal, N.H. Nguyen, J.L. Deenik, Assessing the effects of digestates and combinations of digestates and fertilizer on yield and nutrient use of Brassica juncea(Kai Choy), Agronomy 11 (509) (2021) 1–16, https://doi.org/10.3390/agronomy11030509.
[15] B. Shrestha, R. Hernandez, D.L.B. Fortela, W. Sharp, A. Chistoserdov, D. Gang, E. Revellame, W. Holmes, M.E. Zappi, A review of pretreatment methods to enhance solids reduction during anaerobic digestion of municipal wastewater sludges and the resulting digester performance: implications to future urban biorefineries, Appl. Sci. 0 (2020) 1–28, https://doi.org/10.3390/app10249141.
[16] A.M. Yeneneh, T.K. Sen, S. Chong, H.M. Ang, A. Kayaalp, Effect of combined microwave-ultrasonic pretreatment on anaerobic degradability of primary excess activated and mixed sludge, Comput. Water Energy Environ. Eng. 2 (2013) 7–11.
[17] P. Baredar, S. Suresh, A. Kumar, P. Krishnakumar, A review on enhancement of biogas yield by pre-treatment and addition of additives, in: MATEC Web of Conferences, vol. 62, ICCFE 2016, 2016, 00602, 10.1051matecconf/20166206002.
[18] G. Sodeifian, S.A. Sajadian, N.S. Ardestani, Evaluation of the response surface and hybrid artificial neural network-genetic algorithm methodologies to determine extraction yield of Ferulagoangulatathrough supercritical fluid, J. Taiwan Inst. Chem. Eng. 60 (2016) 165–173.
[19] V.N. Nwobasi, P.K. Igbokwe, C.E. Onu, Optimization of acid activated ngbo clay catalysts in esterification reaction using response surface methodology, Asian J. Phy.Chem. Sci. 10 (1) (2022) 11–27, https://doi.org/10.9734/AJOPACS/2022/v10i130147.

[20] C.H. Ezedinma, N.T. Nwabanne, C.E. Onu, C.O. Nwajinka, Optimum process parameters and thermal properties of moisture content reduction in water yam drying, Asian J. Chem. Sci. 9 (4) (2021) 44–54, https://doi.org/10.9734/AJOCS/2021/v9i419080.

[21] U.I. Onyekwelu, J.T. Nwabanne, C.E. Onu, Characterization and optimization of biodiesel produced from palm oil using acidified clay heterogeneous catalyst, Asian Journal of Applied Chemistry Research 8 (3) (2021) 9–23, https://doi.org/10.9734/AJACR/2021/v8i330192.

[22] C.O. Asadu, C.A. Ezema, C.E. Onu, N.O. Ogbodo, O.I. Maxwell, O.F. Ugwele, A.S. Chukwuebuka, T.O. Onah, E.G. Nwakwasi, I.S. Sunday, E.M. Ezeh, Equilibrium isotherm modelling and optimization of oil layer removal from surface water by organic acid grafted plantain pseudo stem fiber, Case Studies in Chem. Environl. Eng. 5 (2022), 100194, https://doi.org/10.1016/j.cscee.2022.100194, 1 – 12.

[23] S. Gholamhossein, A.S. Seyed, S.A. Nedasadat, Evaluation of the response surface and hybrid artificial neural network-genetic algorithm methodologies to determine extraction yield of ferulagoangulatathrough supercritical fluid, J. Taiwan Inst. Chem. Eng. 60 (2016) 165–173, https://doi.org/10.1016/j.jtice.2015.11.003.

[24] C.E. Onu, P.K. Igbokwe, J.T. Nwabanne, C.O. Nwanjinka, P.E. Ohale, Evaluation of optimization techniques in predicting optimum moisture content reduction in drying potato slices, Artificial intelligence in Agriculture 4 (2020) 39–47, https://doi.org/10.1016/j.aiia.2020.04.001.

[25] N. Bahman, F.A. Sina, Application of ANFIS, ANN, and logistic methods in estimating biogas production from spent mushroom compost (SMC). Resources, Conserv. Recycl. 133 (2018) 169–178, https://doi.org/10.1016/j.resconrec.2018.02.025.

[26] C.E. Onu, P.K. Igbokwe, J.T. Nwabanne, P.E. Ohale, ANFIS, ANN, and RSM modeling of moisture content reduction of cocoyam slices, J. Food Process. Preserv. 46 (1) (2021), e16032, https://doi.org/10.1111/jfpp.16032, pp. 1 - 19.

[27] AOAC, Official Method of Analysis. Association of Official Analytical Chemists, eighteenth ed., AOAC, Washington DC, 2005.

[28] C.E. Onu, et al., Decolourization of bromocresol green dye solution by acid functionalized rice husk: artificial intelligence modeling, GA optimization, and adsorption studies, Journal of Hazardous Materials Advances 9 (2023), 100224, https://doi.org/10.1016/j.hazadv.2022.100224.

[29] E. Gupta, S. Purwar, P. Jaiswal, C.R. Reena, G.K. Rai, Sensory evaluation and nutritional composition of developed papaya-gooseberry jam, Food Nutr. Sci. 7 (2016) 600–608.

[30] P.M. Venkatesh, R. Karthikeyan, Comparative studies on modelling and optimization of hydrodynamic parameters on inverse fluidized bed reactor using ANN-GA and RSM, Alexandria Eng.J. 57 (2018) 3019–3032, https://doi.org/10.1016/j.aej.2018.05.002.

[31] P. Parvaneh, A. Aazam, M. Hojatollah, H.A. Abbas, M.M. Amir, S. Mojtaba, Process modeling and evaluation of petroleum refinery wastewater treatment through response surface methodology and artificial neural network in a photocatalytic reactor using poly ethyleneimine (PEI)/titania (TiO2) multilayer film on quartz tube, Appl. Petrochem Res 5 (2015) 47–59, https://doi.org/10.1007/s13203-014-0077-7.

[32] E.C. Nwadike, M.N. Abonyi, J.T. Nwabanne, P.E. Ohale, Optimization of solar drying of blanched and unblanched aerial yam using response surface methodology, International Journal of Trend in Scientific Research and Development 4 (3) (2022) 659–666. https://www.ijtsrd.com/papers/ijtsrd30598.

[33] L.N. Emembolu, P.E. Ohale, C.E. Onu, N.J. Ohale, Comparison of RSM and ANFIS modeling techniques in corrosion inhibition studies of Aspilia Africana leaf extract on mild steel and aluminium metal in acidic medium, Applied Surface Science Advances 11 (2022), 100316, https://doi.org/10.1016/j.apsadv.2022.100316.

[34] M.J. Prakash, V. Sivakumar, K. Thirugnanasambandham, R. Sridhar, Artificial neural network and response surface methodology modeling in mass transfer parameters predictions during osmotic dehydration of Carica papaya L, Alexandria Eng.J. 53 (2013) 507–516, https://doi.org/10.1016/j.aej.2013.06.007.

[35] R. Mashallah, A. Mosavi, S. Shirazian, ANFIS pattern for molecular membranes separation optimization, J. Mol. Liq. 274 (2019) 470–476, https://doi.org/10.1016/j.molliq.2018.11.017.

[36] M. Mostafaei, H. Javadikia, L. Naderloo, Modeling the effects of ultrasound power and reactor dimension on the biodiesel production yield: comparison of prediction abilities between response surface methodology (RSM) and adaptive neurofuzzy inference system (ANFIS), Energy 115 (2016) 626–636.

[37] C.M. Agu, M.C. Menkiti, P.E. Ohale, V.I. Ugonabo, Extraction modeling, kinetics, and thermodynamics of solvent extraction of Irvingiagabonensis kernel oil, for possible industrial application, Eng. Rep. 12306 (2020), https://doi.org/10.1002/eng2.12306.

[38] P.E. Ohale, O.J. Nwajiobi, C.E. Onu, E.M. Madiebo, N.J. Ohale, Solvent Extraction of Oil from Three Cultivars of Nigerian Mango Seed Kernel: Process Modeling, Optimization and Oil Characterization, Applied Food Research, 2022, https://doi.org/10.1016/j.afres.2022.100227.

[39] Onu, et al., Adsorptive removal of bromocresol green dye using activated corn cob, J. Eng. Appl. Sci. 21 (2022) 1. https://ssrn.com/abstract=4153757.

[40] P.E. Ohale, C.E. Onu, N.J. Ohale, S.N. Oba, Adsorptive kinetics, isotherm and thermodynamic analysis of fishpond effluent coagulation using chitin derived coagulant from waste Brachyura shell, Chemical Engineering Journal Advances 4 (2020), 100036, https://doi.org/10.1016/j.ceja.2020.100036.

[41] A. Das, C. Mondal, Comparative kinetic study of anaerobic treatment of thermally pretreated source-sorted organic market refuse, J. Eng. (2015) 1–14, 684749.

[42] P. Tsapekos, P.G. Kougias, H. Egelund, U. Larsen, J. Pedersen, P. Trenel, I. Angelidaki, Mechanical pretreatment at harvesting increases the bioenergy output from marginal land grasses, Renew. Energy 111 (2017) 914–921.

[43] G.K. Latinwo, S.E. Agarry, Modelling the kinetics of biogas production from mesophilic anaerobic co-digestion of cow dung with plantain peels, Int. J. Renew. Energy Dev. 4 (1) (2015) 55–63.

[44] A. Ali, R.B. Mahar, E.M. Abdelsalam, S.T.H. Sherazi, Kinetic modeling for bioaugmented anaerobic digestion of the organic fraction of municipal solid waste by using Fe_3O_4 nanoparticles, Waste and Biomass Valorization (2018), https://doi.org/10.1007/s12649-018-0375-x.

[45] R. Karki, W. Chuenchart, K.C. Surendra, S. Sung, L. Raskin, S.K. Khanal, Anaerobic co-digestion of various organic wastes: kinetic modeling and synergistic impact evaluation, Bioresour. Technol. 343 (2022), 126063, https://doi.org/10.1016/j.biortech.2021.126063.

[46] Z. Wang, Y. Jiang, S. Wang, Y. Zhang, Y. Hu, Z. Hu, G. Wu, X. Zhan, Impact of total solids content on anaerobic co-digestion of pig manure and food waste: insights into shifting of the methanogenic pathway, Waste Management 114 (2020) 96–106, https://doi.org/10.1016/j.wasman.2020.06.048.

[47] D.R.S. Lima, O.F.H. Adarme, B.E.L. Baêta, L.V.A. Gurgel, S. Francisco de Aquino, Influence of different thermal pretreatments and inoculum selection on the biomethanation of sugarcane bagasse by solid-state anaerobic digestion: a kinetic analysis, Ind. Crop. Prod. 111 (2018) 684–693.

[48] M.O. Ilori, A. Sunday, S.A. Adebusoye, A.K. Lawal, O.A. Awotiwon, Production of biogas from banana and plantain peels, Adv. Environ. Biol. 1 (1) (2007) 33–38.

[49] A.A. Abubakar, Biogas potentials of some selected kitchen wastes within Kaduna metropolis, American J. Eng. Res. (AJER) 6 (5) (2017) 53–63.

[50] A.D. Tambuwal, C. Ogbiko, Proximate and chemical analyses of selected agricultural wastes used for biogas production, Sci. Res. Annals 9 (1) (2018) 56–60.

[51] U.E. Günerhan, L. Dumlu, V. Yılmaz, H. Carrère, A.N. Perendeci, Impacts of chemical-assisted thermal pretreatments on methane production from fruit and vegetable harvesting wastes: process optimization, Molecules 25 (500) (2020) 1–21, https://doi.org/10.3390/molecules25030500.

[52] O.C. Iheanacho, J.T. Nwabanne, C.C. Obi, C.E. Onu, Packed bed column adsorption of phenol onto corn cob activated carbon: linear and nonlinear kinetics modeling, S. African J. Chem. Eng. 36 (2021) 80–93, https://doi.org/10.1016/j.sajce.2021.02.003.

[53] R. Bala, M.K. Mondal, Study of biological and thermo-chemical pretreatment of organic fraction of municipal solid waste for enhanced biogas yield, Environl. Sci. Pollution Res. 27 (2019) 27293–27304, https://doi.org/10.1007/s11356-019-05695-w.

[54] C.O. Iheanacho, J.T. Nwabanne, C.E. Onu, Optimum process parameters for activated carbon production from rice husk for phenol adsorption, Current J. Appl. Sci. Technol. 36 (6) (2019) 1–11, https://doi.org/10.9734/CJAST/2019/v36i630264.

[55] C.E. Onu, J.T. Nwabanne, Application of response surface methodology in malachite green adsorption using nteje clay, Open J. Chem. Eng. Sci. 1 (2) (2014) 19–33.

[56] J.T. Nwabanne, E.C. Okpe, C.O. Asadu, C.E. Onu, Application of response surface methodology in phenol red adsorption using kola nut (cola acuminata) shell activated carbon, Int. Res. J. Pure Appl. Chem. 15 (4) (2017) 1–14, https://doi.org/10.9734/IRJPAC/2017/39421.

[57] C.E. Onu, J.T. Nwabanne, P.E. Ohale, C.O. Asadu, Comparative analysis of RSM, ANN and ANFIS and the mechanistic modeling in eriochrome black-T dye adsorption using modified clay,S, African J. Chem.Eng. 36 (2021) 24–42, https://doi.org/10.1016/j.sajce.2020.12.003.

[58] E.C. Okpe, C.O. Asadu, C.E. Onu, Statistical analysis for orange G adsorption using kola nut shell activated carbon, J. Chinese Adv. Mater. Society 6 (4) (2018) 605–619, https://doi.org/10.1080/22243682.2018.1534607.

[59] M. Nazerian, M. Kamyab, M. Shamsian, M. Dahmardehb, M. Kooshaa, Comparison of response surface methodology (RSM) and artificial neural networks (ANN) towards efficient optimization of flexural properties of gypsum-bonded fiberboards, Cerne 24 (1) (2018) 35–47, https://doi.org/10.1590/01047760201824012484.
[60] E. Betiku, A.S. Osunleke, V.O. Odude, A. Bamimore, B. Oladipo, A.A. Okeleye, N.B. Ishola, Performance evaluation of adaptive neuro-fuzzy inference system, artificial neural network and response surface methodology in modeling biodiesel synthesis from palm kernel oil by transesterification, Biofuels (2018) 1–17, https://doi.org/10.1080/17597269.2018.1472980.
[61] F. Karimi, S. Rafiee, G.A. Taheri, M. Karimi, Optimization of an air drying process for Artemisia absinthiumleaves using response surface and artificial neural network models, J. Taiwan Inst. Chem. Eng. 43 (2012) 29–39, https://doi.org/10.1016/j.jtice.2011.04.005.
[62] M.I. Ejimofor, I.G. Ezemagu, M.C. Menkiti, Biogas production using coagulation sludge obtained from paint wastewater decontamination: characterization and anaerobic digestion kinetics, Current Research in Green and Sustainable Chemistry 3 (2020), 100024, https://doi.org/10.1016/j.crgsc.2020.100024.
[63] C.N. Nweke, J.T. Nwabanne, C.E. Onu, N.V. Ewuzie, Biogas production kinetic studies from yam peels, J. Eng. Applied Sci. 20 (1) (2022) 753–766.
[64] H.M. Poggi-Varaldo, R. Rodriguez-Vazquez, G. Fernandez-Villagomez, F. Esparza-Garcia, Inhibition of mesophilic solid-substrate anaerobic digestion by ammonia nitrogen, Appl. Microbiol. Biotechnol. 47 (3) (1997) 284–291.
[65] P.O. Ebunilo, E.K. Orhorhoro, O.A. Adegbayi, Investigation of the purification of biogas from domestic wastes using local materials in Nigeria, Int.J. Scientific & Eng. Res. 7 (2) (2016) 505–514.
[66] M.D.C. Schiavon, F. Cardozo, L. Frare, M. Gimenes, N. Pereira, Purification of biogas for energy use, Chem. Eng. Transactions 37 (2014) 643–648, https://doi.org/10.3303/CET1437108.
[67] B. Rahmat, I. Hodiyah, A. Supriadi, M. Hikmat, G. Purnama, Design of biogas digester with thermophilic pretreatment for reducing fruits wastes, Int. J. Recycling of Organic Waste in Agric. 8 (1) (2019) S291–S297.
[68] I. Utami, S. Redjeki, D.H. Astuti, A. Sani, Biogas production and removal COD-BOD and TSS from wastewater industrial alcohol (vinasse) by modified UASB bioreactor, MATEC Web of Conferences 58 (2016), 01005, https://doi.org/10.1051/matecconf/20165801005. BISSTECH2015.
[69] I. Kouzi, M. Puranen, M.H. Kontro, Evaluation of the factors limiting biogas production in full-scale processes and increasing the biogas production efficiencies, Environ. Sci. Pollut. Res. 27 (2020) 28155–28168, https://doi.org/10.1007/s11356-020-09035-1.